J. Fluid Mech. (1991), *vol.* 229, *pp.* 555–567
Printed in Great Britain

Particle orbits in a rotating liquid

By GLYN O. ROBERTS[1], DALE M. KORNFELD[2] AND WILLIAM W. FOWLIS[2]

[1] Roberts Associates, Incorporated, 11794 Great Owl Circle, Reston, VA 22094–1173, USA

[2] Space Science Laboratory, Code ES74, NASA Marshall Space Flight Center, Huntsville, AL 35812, USA

(Received 15 September 1987 and in revised form 25 January 1991)

Monodisperse latex microspheres ranging in size from submicrometer to several micrometers in diameter can be prepared in the laboratory. The uniformity of diameter is important for instrument calibration and other applications. However it has proved very difficult to manufacture commercial quantities of mondisperse latex microspheres with diameters larger than about 3 micrometers owing to buoyancy and sedimentation effects. In an attempt to eliminate these effects NASA sponsored a Space Shuttle experiment called the Monodisperse Latex Reactor (MLR) to produce these monodisperse microspheres in larger sizes in microgravity. Results have been highly successful.

Using technology gained from this space experiment, a ground-based rotating latex reactor has been fabricated in an attempt to minimize sedimentation without using microgravity. The entire reactor cylinder is rotated about a horizontal axis to keep the particles in suspension.

In this paper we determine the motion of small spherical particles under gravity, in a viscous fluid rotating uniformly about a horizontal axis. The particle orbits are approximately circles, with centres displaced horizontally from the axis of rotation. Owing to net centrifugal buoyancy, the radius of the circles increases (for heavy particles) or decreases (for light particles) with time, so that the particles gradually spiral inward or outward.

For a large rotation rate, the particles spiral outwards or inwards too fast, while for a small rotation rate, the displacement of the orbit centre from the rotation axis is excessive in relation to the reactor radius. We determine the rotation rate that maximizes the fraction of the reactor cross-section area that contains particles that will not spiral out to the wall in the experimental time (for heavy particles), or that have spiralled in without hitting the wall (for light particles). Typically, the rate is close to 1 r.p.m., and design rotation rate ranges should span this value.

1. Introduction

There is a need for microscopic spherical particles of an extremely uniform (monodisperse) size. These particles, called microspheres, are used as calibration standards for optical and electron microscopes, and for many other scientific purposes. Since 1947 monodisperse polystyrene latexes have been widely used for these applications (Vanderhoff 1964).

These early particles ranged in size from submicrometer to several micrometers (μm) in diameter. Over the years, as larger polystyrene microspheres were prepared, a major difficulty in their manufacture was that amounts of coagulum produced

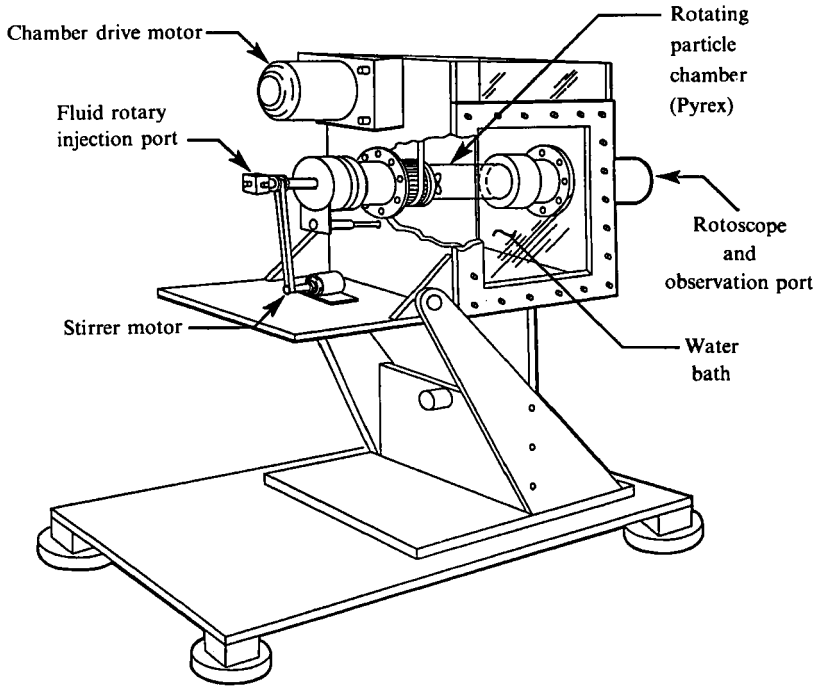

FIGURE 1. A prototype Rotary Reactory to minimize gravitational settling (or creaming) for the growing latex particles.

always increased along with size, giving complete coagulum instead of particles in the size range greater than about 10 μm. Attempts to adjust the chemistry of the latex to reduce coagulum usually resulted in the production of a non-monodisperse latex, contaminated with particles of other sizes (Vanderhoff, El-Aasser & Micale 1978).

The main causes of these problems were buoyancy and sedimentation effects. During the early stages of a seeded emulsion polymerization reaction using standard techniques and equipment, the large monomer-swollen latex seed particles tend to rise to the surface of the mixture (cream) because the average density of the particles is less than that of the water medium in which they are suspended. During the later stages of the polymerization, the growing seed particles become heavier as more lower-density monomer is converted to higher-density polymer, and they settle to the bottom of the reactor. As the particles are grown to sizes larger than about 2 μm (at which size they show only little Brownian motion) the rates of creaming and settling become so rapid that it is not possible to keep the particles in suspension using conventional paddle or propellor-type stirrers without resorting to excessive agitation rates. The growing particles are soft and sticky, and increasing the stirring rate causes more violent particle–particle collisions, resulting in flocculation. Since agitating the particles at rates high enough to prevent creaming or settling also results in flocculation, a different method of agitation had to be developed to produce these larger-size monodisperse latex particles. Another possible solution was to put the particles in an environment in which no stirring was needed.

Because this difficulty in producing usable quantities of monodisperse polystyrene latex particles in sizes greater than about 3 μm is gravity related, NASA sponsored a research effort to determine whether it would be possible to manufacture them in the microgravity environment of space.

This effort resulted in the highly successful Monodisperse Latex Reactor (MLR) Space Processing Experiment, which has now been flown into Earth orbit on five space shuttle missions. With Dr John W. Vanderhoff of Lehigh University as the principal investigator, this MLR experiment has successfully produced large-particle monodisperse polystyrene latexes up to 30 μm in diameter with coefficients of variation of less than 1% (Vanderhoff *et al.* 1987).

The 10 μm and 30 μm microspheres manufactured aboard the Space Shuttle are currently being marketed by the US National Bureau of Standards as Standard Reference Material (SRM) 1960 and SRM 1961 respectively. These are the first products ever manufactured in space to be commercially marketed on Earth (Kornfeld 1985; US Patent No. 4247434).

During the course of the space experiments, one of the authors (D.M.K., who is also NASA Co-Investigator with Dr Vanderhoff on the MLR experiment) proposed that, as part of the supporting ground-based research, the same seeded emulsion polymerization recipes currently being used in space also be tested in a laboratory rotating-cylinder reactor. He then designed and fabricated a prototype Rotary Reactor (figure 1) to minimize gravitational settling on Earth for the growing latex particles.

In this apparatus a cylindrical polymerization reactor chamber is rotated about its horizontal axis within a water bath. The Rotary Reactor is designed to maintain uniformity in particle concentration and temperature profile with minimal or no stirring. The particles are kept in suspension only through the rotation of the reactor; the slow rotation of the entire chamber during polymerization helps to prevent the growing particles from either creaming or settling. Once steady rotation of the seed latex mixture is achieved in this apparatus, there is no agitation to cause the violent particle collisions that result in flocculation.

It has already been established experimentally that large-size latex particles up to 100 μm diameter can be successfully suspended and polymerized at low reactor rotation rates. Particles manufactured thus far in this prototype reactor have exhibited coefficients of variation inferior to those produced in the Space Shuttle, but it is expected that latex quality will improve as latex recipes are optimized for this type reactor and optimum rotation rates are determined for each particle size and latex recipe.

As mentioned earlier, the density of the seed latex particles increases with time, through the conversion of the low-density styrene monomer into the higher-density polystyrene polymer, so the growing particles undergo a constant increase in density throughout the course of the reaction. While slowly rotating in this manner the particles are strongly influenced by viscous drag and tend to rotate with the fluid medium. Their motion relative to the rotating fluid is determined by a balance of their gravitational and centrifugal forces with the viscous drag, and the sign of the buoyancy forces depends on the density difference between the particles and the fluid.

At higher rotation rates, more-dense particles will tend to be centrifuged outward and deposited on the cylinder wall of the Rotary Reactor. Less-dense particles will be centrifuged inwards and will form a mass near the axis. A lower limit on the rotation rate is determined by the time it takes the particles to fall through (or rise through) a distance close to the radius of the reactor cylinder. Clearly there is an optimization problem for the rotation rate.

In this paper the particle orbits in the Rotary Reactor are determined, and the optimization problem is solved with the assumption that the particle density and

radius remain fixed. Section 2 contains the formulation and solution of the particle orbit problem and §3 contains the formulation and solution of the rotation rate optimization problem. In §4 the principal conclusions are stated.

2. Formulation and solution of the problem for particle orbits

Basic mechanisms for the suspension of heavy particles in a rotating cylinder of fluid were discussed by Otto & Lorenz (1978) but a formal solution was not obtained. A more complete study of the particle orbit problem was presented by Schatz (1977), but the centrifugal buoyancy was not handled correctly. Related studies by Dill & Brenner (1983), Nadim, Cox & Brenner (1985), Aoki *et al.* (1986) and Annamalai & Cole (1983), addressed parts of the problem. In their later work, Annamalai & Cole (1987) obtained an orbit solution essentiallly equivalent to ours, in the context of bubbles. None of these references analysed the optimization problem studied here.

In this section the particle orbit problem is correctly solved. The ambient fluid is taken to be in solid-body rotation about the horizontal z-axis through the origin (see figure 2) with rotation rate Ω. Then the fluid flow in the (x, y)-plane is given by

$$\boldsymbol{u} = \boldsymbol{\Omega} \times \boldsymbol{x} = (-\Omega y, \Omega x). \tag{1}$$

The corresponding pressure distribution is

$$p = p_0 + \rho_f(\tfrac{1}{2}\Omega^2 r^2 - gy), \tag{2}$$

where p_0 is a constant, ρ_f is the fluid density and $r^2 = x^2 + y^2$, so that r is the cylindrical radius coordinate. The gradient of this pressure balances the gravitational and centrifugal forces on the fluid.

The vector equation of motion for a spherical particle of radius a, density ρ_p, volume V, and mass M at position $\boldsymbol{x}$ is

$$M\boldsymbol{x}'' = -Mg\hat{\boldsymbol{y}} + \boldsymbol{P} + \boldsymbol{D}, \tag{3}$$

where the stress forces exerted by the fluid on the particle have been separated into a pressure force $\boldsymbol{P}$ and a drag force $\boldsymbol{D}$. The prime and double prime are used to denote the first and second time derivatives.

The pressure force is defined as

$$\boldsymbol{P} = -\int p \, \mathrm{d}\boldsymbol{S}, \tag{4}$$

where p is the fluid pressure given by equation (2) above, and the integration is over the particle surface. Using the Gauss theorem,

$$\boldsymbol{P} = \rho_f V(-\Omega^2 x, g - \Omega^2 y). \tag{5}$$

The g-term is the familiar Archimedes buoyancy force. The Ω^2 term is the corresponding inward pressure gradient which would cancel the centrifugal acceleration of the liquid which the particle has displaced. This term was apparently omitted by Schatz (1977).

The drag force is written using the Stokes slow-flow approximation. In this viscous limit

$$\boldsymbol{D} = -6\pi\eta a(\boldsymbol{x}' - \boldsymbol{\Omega} \times \boldsymbol{x}) \tag{6}$$

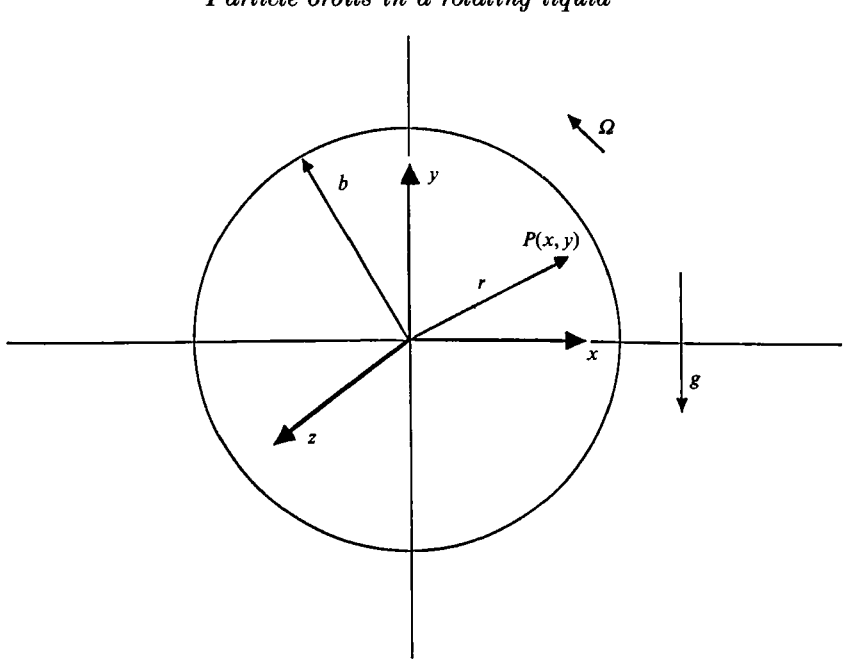

FIGURE 2. Schematic view along the axis of symmetry of the Rotary Reactor showing the coordinate system used.

where η is the fluid viscosity. The drag force opposes the motion of the particle relative to the fluid. The approximation requires that the Reynolds number and the Taylor number be much smaller than unity, where

$$Re = \rho_f a V/\eta, \tag{7}$$

$$Ta = \rho_f a^2 \Omega/\eta, \tag{8}$$

and V is the relative motion of the particle ($V = |\boldsymbol{x}' - \boldsymbol{\Omega} \times \boldsymbol{x}|$).

Combining these expressions, the two non-trivial components of the equation of motion can be written as

$$x'' + cx' + \frac{\rho_f}{\rho_p}\Omega^2 x + c\Omega y = 0, \tag{9}$$

$$y'' + cy' + \frac{\rho_f}{\rho_p}\Omega^2 y - c\Omega x = -\frac{\Delta\rho}{\rho_p} g, \tag{10}$$

where the drag constant,

$$c = \frac{9\eta}{2\rho_p a^2}, \tag{11}$$

is the rate at which motion decays through drag forces alone and $\Delta\rho = \rho_p - \rho_f$. The term on the right-hand side of (10) arises from the particle weight less the Archimedes buoyancy force. The Ω^2 terms on the left-hand sides of (9) and (10) arise from the centrifugal pressure term in (5).

The coupled x- and y-equations can be solved conveniently by introducing the complex variable

$$w = x + \mathrm{i}y. \tag{12}$$

Multiplying (10) by i and adding (9) gives the complex, second-order, linear equation

$$w''+cw'+\left(\frac{\rho_f}{\rho_p}\Omega^2-ic\Omega\right)w=-i\frac{\Delta\rho}{\rho_p}g. \tag{13}$$

The general solution of (13) is the sum of a particular integral and a complementary function

$$w=w_0+A_1\exp(m_1t)+A_2\exp(m_2t). \tag{14}$$

For this problem the particular integral is the constant

$$w_0=x_0+iy_0=\frac{\Delta\rho g}{\rho_p c\Omega}\left(1+i\frac{\rho_f}{\rho_p}\frac{\Omega}{c}\right)^{-1}. \tag{15}$$

The real and imaginary parts represent the equilibrium position of the particle in the (x,y)-plane. The complex constants m_1 and m_2 are the roots of the quadratic auxiliary equation

$$m^2+cm+\left(\frac{\rho_f}{\rho_p}\Omega^2-ic\Omega\right)=0. \tag{16}$$

The complex constants A_1 and A_2 are determined by the initial values $w(0)$ and $w'(0)$ at time zero, using the equations

$$A_1+A_2=w(0)-w_0, \tag{17}$$

$$m_1A_1+m_2A_2=w'(0). \tag{18}$$

These simultaneous equations can be easily solved for A_1 and A_2.

The general solution (14) represents the superposition of two spiral motions about the equilibrium position (x_0,y_0). Consider the solution

$$w=x+iy=A_1\exp(m_1t), \tag{19}$$

where

$$A_1=\alpha\exp(i\theta), \tag{20}$$

$$m_1=m_r+im_i. \tag{21}$$

Here α is the positive amplitude of A_1 and θ is its phase, while m_r and m_i are the real and imaginary part of m_1. The real and imaginary parts of w are

$$x=\alpha e^{m_rt}\cos(m_it+\theta), \tag{22}$$

$$y=\alpha e^{m_rt}\sin(m_it+\theta). \tag{23}$$

The instantaneous spiral radius is αe^{m_rt}, and grows or decays exponentially depending on the sign of m_r. The phase angle $m_it+\theta$ determines the direction of the vector displacement (x,y) in the (x,y)-plane.

We now use the inequality

$$\Omega \ll c. \tag{24}$$

Note that for $\eta\sim10^{-2}$ g/cm s^{-1}, $\rho_p\sim1$ g/cm^3 and $a\sim10^{-3}$ cm (corresponding to a diameter of 20 μm), c is 4.5×10^4 s^{-1}. Thus even for much larger radii, this assumption is valid for a very wide range of practical rotation rates.

Using this approximation, the spiral centre (15) is at

$$w_0=x_0+iy_0=\frac{g\Delta\rho}{\Omega c\rho_p}=\frac{2ga^2\Delta\rho}{9\eta\Omega}, \tag{25}$$

so that the spirals are centred about a point on the x-axis, displaced horizontally from the axis of rotation. At this point the drag force balances the net weight. Naturally, this point must be inside the rotating reactor, since if the point is outside or on the rotating reactor wall all the particle orbits will strike the wall. This puts a lower limit on Ω:

$$\Omega > \Omega_{\min} = \frac{g|\Delta\rho|}{bc\rho_p} = \frac{2ga^2|\Delta\rho|}{9\eta b}, \tag{26}$$

where b is the radius of the rotating reactor. For $|\Delta\rho|/\rho_p \sim 0.1$, $g \sim 10^3$ cm/s^2, $b \sim 3.0$ cm and for the above value for c, $\Omega_{\min}$ is 7.4×10^{-4} s^{-1}, cf. table 2.

Using the assumption (24), the two roots of the quadratic equation (16) can be approximated as

$$m_1 = \mathrm{i}\Omega + d, \tag{27}$$

$$m_2 = -c - \mathrm{i}\Omega, \tag{28}$$

where the growth or decay rate for the first spiral, in (27), is

$$d = \frac{\Delta\rho}{\rho_p}\frac{\Omega^2}{c}, \tag{29}$$

which is real and much less than Ω. Note that for the second spiral, the real part is $-c$, so that the radius decreases exponentially on the very short drag timescale, $1/c$. Thus the second spiral solution becomes negligibly small in a few drag timescales, for any realistic initial conditions. The full general solution therefore can be approximated as

$$x = x_0 + \alpha\, \mathrm{e}^{dt} \cos(\Omega t + \theta), \tag{30}$$

$$y = \alpha\, \mathrm{e}^{dt} \sin(\Omega t + \theta), \tag{31}$$

where α and θ are determined by the initial displacement from the centre of the spiral.

Note that the radius of the displacement from the spiral centre is $\alpha\, \mathrm{e}^{dt}$, where d is much less than Ω and has the sign of $\Delta\rho$. The rotation rate of the spiral is Ω, so the particle rotates about the centre of the spiral at the same rate as the fluid rotates about the axis. The exponent for growth or decay of the radius during the experimental time T is

$$\epsilon = |d|\, T = \frac{|\Delta\rho|\, \Omega^2 T}{\rho_p c}. \tag{32}$$

Whether $\Delta\rho$ is positive or negative, we will normally require that the exponent ϵ is of order unity or less, for otherwise either most of the particles spiral out to the boundary of the reactor or they spiral in until their concentration is excessive. Thus we require

$$\Omega^2 < \Omega^2_{\max} = \frac{\rho_p c}{|\Delta\rho|\, T} = \frac{9\eta}{2a^2 T|\Delta\rho|}. \tag{33}$$

For $T = 10^5$ s, or slightly longer than a day, the upper limit for Ω using the previous assumptions is 2.12 s^{-1}.

Physically, the spiralling in or out is caused by the centrifugal force less the inward centrifugal pressure force. That is why it has the sign of $\Delta\rho$. This force is balanced by the drag force to determine the rate of spiralling inwards or outwards.

By equating the lower and upper limits, (26) and (33), for Ω, we can obtain an approximate upper limit for the radius of the particles for the rotating reactor to be useful,

$$a_{\max}^6 = \left(\frac{9\eta}{2|\Delta\rho|}\right)^3 \frac{b^2}{g^2 T}. \tag{34}$$

Using $\eta \sim 10^{-2}$ g/cm s^{-1}, $|\Delta\rho| = 0.1$ g/cm^3, $b = 3$ cm, $g = 10^3$ cm/s^2 and $T = 10^5$ s, as before, we obtain $a_{\max}$ as 1.42×10^{-2} cm, corresponding to a diameter of 284 μm. This upper limit is discussed further in the following section.

3. Optimization of the rotation rate

From the previous section, the choice of the rotation rate involves the following dimensionless variables:

$$\delta = \frac{|x_0|}{b} = \frac{\Omega_{\min}}{\Omega} = \frac{2ga^2|\Delta\rho|}{9b\eta\Omega}, \tag{35}$$

$$\epsilon = \frac{\phi^3}{2\delta^2} = \left(\frac{\Omega}{\Omega_{\max}}\right)^2 = \frac{2a^2T|\Delta\rho|\,\Omega^2}{9\eta}. \tag{36}$$

Here we have introduced the dimensionless quantity ϕ^3, independent of the rotation rate, and defined by the relations

$$\begin{aligned}\phi^3 &= 2\epsilon\delta^2 \\ &= 2(\Omega_{\min}/\Omega_{\max})^2 \\ &= 2(a/a_{\max})^6 \\ &= 2a^6g^2Tb^{-2}(2|\Delta\rho|/9\eta)^3.\end{aligned} \tag{37}$$

The definition using ϕ^3, and the factor 2, are for later convenience.

The limit $\Omega_{\min}$ corresponds to the strict requirement

$$\delta < 1, \tag{38}$$

so that the spiral centre is inside the rotating reactor. The limit $\Omega_{\max}$ corresponds to the loose requirement

$$\epsilon \lesssim 1, \tag{39}$$

so that the centrifugal spiralling is not excessive during the period T. The radius changes by a factor e^{ϵ} during this time interval.

An optimization problem can be defined for both signs of the particle density excess $\Delta\rho$. For positive $\Delta\rho$, the particles spiral outward, and we maximize the fraction F of the reactor cross-section area for which particles starting there will not hit the reactor wall in the time interval T. For negative $\Delta\rho$, the particles spiral inwards, and we maximize the fraction F of the reactor cross-section area containing particles which have not hit the wall in the preceding time interval T. T is much more than a rotation period, and is taken as 10^5 s (or 27.8 h) for our examples. Note that this analysis makes no use of the loose inequality (33).

In both cases, the area involved is a circle with its centre at the spiral centre. The distance from the spiral centre to the cylinder wall is $(b-|x_0|)$. The radius of the circle is therefore

$$r_F = (b-|x_0|)\,e^{-\epsilon}. \tag{40}$$

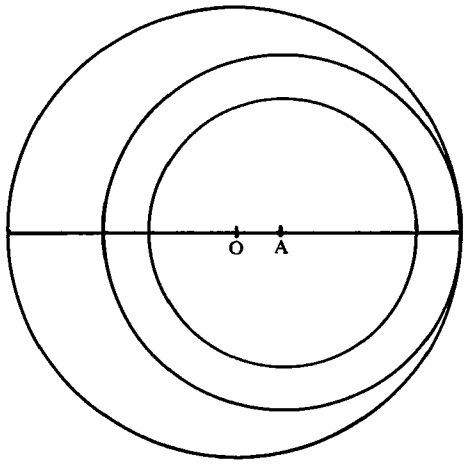

FIGURE 3. Cross-section of the rotary reactor. Heavy or light particles at A are stationary, supported against gravity by the counterclockwise or clockwise flow around the centre O. Other particles move around A in circles, spiralling slowly outward or inward. Particles in the crescent hit the wall on the first cycle. Heavy particles initially between the concentric circles spiral out to hit the wall in time T. Heavy particles in the inner circle spiral out to fill the outer circle. Light particles initially filling the outer circle fill the inner circle after time T. In both cases we choose the rotation rate to maximize the area of the inner circle.

The fraction F is the ratio of the area of this circle (the smallest circle in figure 3) to the cylinder cross-section area (the largest circle). Thus

$$F = \frac{\pi r_F^2}{\pi b^2} = (1-\delta)^2 \, \mathrm{e}^{-2\epsilon}$$

$$= (1-\delta)^2 \exp(-\phi^3/\delta^2). \tag{41}$$

In this last expression for F, ϕ^3 remains constant while Ω and δ vary. F is maximized by differentiation with respect to δ and setting the derivative to zero. Hence

$$\frac{\delta^3}{1-\delta} = \phi^3. \tag{42}$$

This is a cubic equation in δ, with a single solution in the allowed interval $0 < \delta < 1$, for all positive ϕ-values. Approximate analytic solutions for δ can be obtained when ϕ is either very small or very large; otherwise numerical or graphical methods can be used, or δ can be obtained using table 1 as described below.

Once the optimum δ and F have been found, for a particular set of rotating reactor parameters determining the ϕ^3 value (37), the optimum rotation rate is given by (35), in the form

$$\Omega = \Omega_{\min}/\delta. \tag{43}$$

Using (42), with the definitions (35) and (37), this can be written as the alternative form

$$\Omega = \Omega_{\mathrm{s}}(1-\delta)^{-\frac{1}{3}}, \tag{44}$$

where

$$\Omega_{\mathrm{s}} = \frac{\Omega_{\min}}{\phi} = \left(\frac{g}{2bT}\right)^{\frac{1}{3}} \tag{45}$$

is independent of the particle size and density, and of the fluid properties. For our

δ	ϕ^3	$e^{-\epsilon}$	F	$(1-\delta)^{-\frac{1}{3}}$	δ	ϕ^3	$e^{-\epsilon}$	F	$(1-\delta)^{-\frac{1}{3}}$
0.05	0.000 13	0.974	0.856	1.017	0.50	0.250	0.6065	0.0920	1.260
0.10	0.001 11	0.946	0.725	1.036	0.55	0.370	0.5427	0.0597	1.305
0.15	0.003 97	0.916	0.606	1.056	0.60	0.540	0.4724	0.0357	1.357
0.20	0.0100	0.882	0.498	1.077	0.65	0.785	0.3851	0.0191	1.419
0.25	0.0209	0.846	0.403	1.101	0.70	1.143	0.3114	0.0087	1.494
0.30	0.0386	0.807	0.319	1.126	0.75	1.687	0.2231	0.0031	1.587
0.35	0.0660	0.764	0.247	1.154	0.80	2.560	0.1353	0.0007	1.710
0.40	1.1067	0.717	0.185	1.186	0.85	4.094	0.0588	0.0001	1.882
0.45	0.1657	0.664	0.133	1.221	0.90	7.290	0.0111	10^{-6}	2.154

Parameter	Equation	Explanation
δ	(35)	Spiral centre, scaled by the reactor radius b, for the optimized rotation rate.
ϕ^3	(37)	Problem parameter, proportional to sixth power of the particle radius a.
$e^{-\epsilon}$	(36)	Spiral radius changes by factor e^{ϵ} during time T.
F	(41)	Area occupied by particles not interacting with reactor wall during time T, as a fraction of reactor cross-section: maximized value.
$(1-\delta)^{-\frac{1}{3}}$	(44)	Optimum rotation rate, scaled by $\Omega_s = (g/2bT)^{\frac{1}{2}}$.

TABLE 1. Parameter values corresponding to uniformly spaced δ-values

example, with $g = 10^3$ cm/s^2, $b = 3$ cm, and $T = 10^5$ s, Ω_s is 0.118 s^{-1} or 1.132 r.p.m. The expression (45) is useful, because $(1-\delta)^{-\frac{1}{3}}$ does not increase significantly from unity until δ approaches unity.

For the easy case of very small ϕ, Ω_{min} is much less than Ω_{max}. The approximate analytic solution is

$$\delta = \phi, \quad \epsilon = \tfrac{1}{2}\phi, \quad F = 1-3\phi. \tag{46}$$

The corresponding optimum rotation rate for small ϕ is

$$\Omega = \Omega_s(1+\tfrac{1}{3}\phi), \tag{47}$$

or approximately Ω_s. The rotation rate is independent of the particle and fluid properties so long as they ensure that ϕ is small.

The example introduced in the previous section leads to a very small ϕ-value. Using those values,

$$\left.\begin{aligned} \Omega_{min} = 7.4\times10^{-4}\ \text{s}^{-1}, \quad \Omega_{max} = 2.12\ \text{s}^{-1}, \quad \phi^3 = 2(\Omega_{min}/\Omega_{max})^2 = 2.44\times10^{-7}, \\ \delta = \phi = 0.006\,25, \quad \epsilon = \tfrac{1}{2}\phi = 0.003\,12, \quad F = 1-3\phi = 0.9813. \end{aligned}\right\} \tag{48}$$

The optimum rotation rate is accurately given by (47), and is almost exactly Ω_s. The spiral centre is at

$$|x_0| = b\delta = 0.019\ \text{cm}, \tag{49}$$

which is an imperceptible displacement from the reactor axis.

On the other hand, the approximate solution for large ϕ is

$$\delta = 1-\phi^{-3}, \quad \epsilon = \tfrac{1}{2}\phi^3, \quad F = \phi^{-6}\exp(-\phi^3). \tag{50}$$

This is the difficult case of large particles, with Ω_{min} much greater than Ω_{max}. The optimum Ω is only slightly larger than Ω_{min}, and the particles centrifuge so rapidly that the fraction F is exponentially small, and the Rotary Reactor is in effect useless.

For intermediate values of ϕ^3, as given by (37), the use of table 1 may be preferable to solving the cubic equation (42), particularly since F is insensitive to δ near the

optimum value. The table shows optimal values of δ spaced uniformly from zero to one, with the corresponding values of

$$\phi^3 = \frac{\delta^3}{1-\delta}, \quad \epsilon = \frac{\phi^3}{2\delta^2}, \quad F = (1-\delta)^2 \mathrm{e}^{-2\epsilon}, \quad (1-\delta)^{-\frac{1}{3}}.$$

The table can be used, with hand interpolation, to determine values for the other parameters, assuming an optimized rotation rate, for any value of ϕ^3 (or of ϵ or F).

To illustrate the application of table 1, consider the example given in the previous section where the radius is calculated using $\Omega_{\max} = \Omega_{\min}$. This gives in succession

$$a = a_{\max} = 1.42 \times 10^{-2} \text{ cm}, \quad \Omega_{\max} = \Omega_{\min} = 2^{\frac{1}{3}}\Omega_s = 0.1494 \text{ s}^{-1},$$

$$\phi^3 = 2, \quad \delta = 0.77, \quad \epsilon = \frac{\phi^3}{2\delta^2} = 1.68,$$

$$F = (1-\delta)^2 \mathrm{e}^{-2\epsilon} = 0.0018, \quad \Omega = \frac{\Omega_{\min}}{\delta} = \frac{\Omega_s}{(1-\delta)^{\frac{1}{3}}} = 0.1939 \text{ s}^{-1}.$$

Here δ is obtained from ϕ^3 by interpolation in the table, and ϵ and F are then obtained from the formulae. The fraction F of the particles not hitting the wall is unacceptably small, even at the optimum rotation radius.

To determine the largest radius for which a fraction F of 0.5 can be obtained, we again look at the table, and obtain approximately,

$$\delta = 0.2, \quad \phi^3 = 0.01.$$

From (37), $$(a/a_{\max})^6 = \tfrac{1}{2}\phi^3 = (0.4135)^6,$$

which gives a radius limit of 5.9×10^{-3} cm (corresponding to a diameter of 117 μm) for our example. The corresponding optimum rotation rate is

$$\Omega_s/(1-\delta)^{\frac{1}{3}} = 0.1278 \text{ s}^{-1}.$$

4. Conclusions

A rotary reactor is a cylinder of fluid rotating about its horizontal axis in order to keep particles in suspension. Such a reactor has been used to produce larger latex microspheres in the laboratory without flocculation, with results approaching those obtained in space.

An accurate solution for the path followed by a particle in a rotating reactor has been obtained. The path depends on whether the particle is heavier or lighter than the fluid. For counterclockwise rotation, a heavy particle spirals outwards around a spiral centre displaced to the right of the axis. A light particle spirals inwards around a centre displaced to the left. The spiral rotation rate is the same as the rotation rate of the reactor. The relative change in the radius, for each spiral rotation, is very small.

Physically, the horizontal displacement of the spiral centre from the axis of rotation is determined by the condition that the net weight or buoyancy should balance the viscous drag from the fluid flow past the particle. The spiralling outwards or inwards is due to the centrifugal buoyancy (i.e. the centrifugal force on the particle as compared with the centrifugal force on the fluid it displaces).

There are two constraints on the rotation rate of the reactor. It must exceed the minimum value (26), to keep the spiral centre inside the reactor. And it must not be

much larger than the maximum value (33), since either too many particles hit the reactor wall or the particle concentration becomes excessive (for light particles spiralling inwards).

For both cases, there is a natural optimization problem, to choose the rotation rate to maximize the fraction of the reactor cross-section area which contains particles which either will not spiral out to the reactor wall during the experimental time, or have spiralled in without hitting the wall.

The optimization problem was solved to determine the optimum rotation rate and the corresponding fraction value for any set of parameters. Remarkably, the optimum rotation rate is independent of the particle and fluid properties for small particles, and increases only a little as the particle size increases.

Table 2 presents the parameter values for the three examples used in the text. The fluid properties, density difference, reactor diameter, and experimental time are the same in each case. Particle diameters of 20, 284, and 117 μm are considered. The computed rotation rates are presented in r.p.m. units for engineering convenience. The optimum rotation rate maximized the success fraction F of the reactor cross-section area. The spiral centre displacements (from the reactor axis) are shown. The distance of each particle from the spiral centre changes by the indicated factor during the experimental time.

For the first column of values, the particle diameter was chosen as a typical value of interest. The minimum rotation rate is much less than the nominal maximum, and a high success fraction is obtained, with a small spiral-centre displacement and a radius change factor close to unity.

In the second values column, the particle diameter was chosen to make the maximum and minimum rotation rates equal. The optimum rotation rate is somewhat higher, the spiral centre is near the reactor wall, the radius changes by a factor of over five, and the success fraction is very small.

For the third column, the particle diameter was chosen to give a success fraction of a half. The other parameter values are shown.

The time T in the table is roughly appropriate for latex microsphere processing. Note that the optimum rotation rate given by (44) and (45) varies only with the one-third power of g/bT, and is practically independent of the particle radius and density, provided (37) is small. Thus the optimum rotation rate is close to 1 r.p.m. for latex microspheres, and is probably between 0.1 and 10 r.p.m. for a very wide range of microgravity simulations.

Further work is required for a full application of this analysis to the production of monodisperse latex microspheres. As described in §1, the monomer-swollen seed particles are buoyant in the early stages, and converge on the spiral centre. In the later stages, the particles shrink slightly and become heavier than water, and the spiral centre crosses the axis. The heavier particles centrifuge out as the polymerization approaches completion.

The risk and extent of coagulum formation during this process, and the deviations from a monodisperse size distribution due to variations in the particle distribution, are unknown. It can be expected that even if the particles collide near the spiral centre as they centrifuge in during the early stages, the forces between the particles will be much smaller than for particles creamed to the top in a non-rotating reactor. This is because the centrifugal accelerations are extremely small. Thus coagulum formation might be minimal. In the late stages, as particles centrifuge out and hit the wall, there will be further particle collisions, with again the possibility of coagulum formation or size dispersion.

Quantity	Symbol	Values			Unit
Particle diameter	$2a$	20	284	117	μm
Water viscosity	η	0.01	0.01	0.01	g/cm s^{-1}
Water density	ρ_f	1	1	1	g/cm^3
Density difference	$\Delta\rho$	0.1	0.1	0.1	g/cm^3
Reactor diameter	$2b$	6	6	6	cm
Experimental time	T	10^5	10^5	10^5	s
Rotation rate minimum	Ω_{min}	0.0071	1.43	0.243	r.p.m.
Nominal rotation rate maximum	Ω_{max}	20.2	1.43	8.43	r.p.m.
Optimal rotation rate	Ω	1.13	1.85	1.22	r.p.m.
Spiral centre displacement	x_0	0.019	2.31	0.60	cm
Radius change factor	$e^{-\epsilon}$	0.997	0.186	0.882	—
Optimized success fraction	F	0.981	0.0018	0.500	—

TABLE 2. Typical parametric values to illustrate rotation rate limits

A further issue for study involves the beginning of production, and the dynamics and thermodynamics of raising the temperature, with or without stirring. The stirring could also be continued into the polymerization stage.

Finally, we assumed that the solid-body rotation of the fluid is not disturbed by the presence of the particles. However, recent experiments by Kornfeld show significant secondary flows driven by concentration variations, for 0.3% suspensions of 50 μm latex particles, at rotation rates below 1 r.p.m. The dependence of this phenomenon on concentration is weak, while its dependence on rotation rate is very abrupt; at 1.4 r.p.m. there is no observable modification from uniform rotation, while at 0.7 r.p.m. the flow field and particle distribution are totally different. We plan further study of this effect.

Dr William Fowlis died in December 1988.

REFERENCES

ANNAMALAI, A. & COLE, R. 1983 *Adv. Space Res.* **3**, 165.

ANNAMALAI, A. & COLE, R. 1987 *Adv. Space Res.* **8**, 321.

AOKI, A., SHIRANE, K., TOKIMOTO, T. & NAKAGAWI, K. 1986 *Rev. Sci. Instrum.* **57**, 2859.

DILL, L. H. & BRENNER, H. 1983 *J. Colloid Interface Sci.* **94**, 430.

KORNFELD, D. M. 1985 Monodisperse latex reactor – a materials processing space shuttle mid-deck payload. *NASA TM*-86487.

NADIM, A., COX, R. G. & BRENNER, H. 1985 *Phys. Fluids* **28**, 3457.

OTTO, G. H. & LORENZ, A. 1978 Simulation of low gravity conditions by rotation. *AIAA Paper* 78-273.

SCHATZ, A. 1977 Problems of 0-g Simulation With the Fast-Running Clinostat. *Institute for Aerospace Medicine, Cologne, Germany.*

US PATENT No. 4,247,434; issued January 27, 1981, 'Process for Preparation of Large-Particle-Size Monodisperse Latexes'. Inventors: Vanderhoff, J. W., Micale, F. J., El-Aasser, M. S. and Kornfeld, D. M.

VANDERHOFF, J. W. 1964 *Organic Coatings Plastics Chem.* **24**, 223.

VANDERHOFF, J. W., EL-AASSER, M. S., KORNFELD, D. M., MICALE, F. J., SUDOL, E. D., TSENG, C.-M. & SHEU, H.-R. 1987 *Mater. Res. Soc. Symp. Proc.* **87**, 213–223.

VANDERHOFF, J. W., EL-AASSER, M. S. & MICALE, F. J. 1978 *Abstracts, 175th ACS Meeting, Anaheim, CA, March 13–17*, COLL-110.